View metadata, citation and similar papers at core.ac.uk
brought to you by CORE
provided by Covenant University Repository

International Journal of Scientific & Engineering Research, Volume 5, Issue 3, March-2014 1220
ISSN 2229-5518

Facile Route to Synthesize Organically Capped Size Controlled Silver Nanoparticles

Joseph A. Adekoya*, Enock O. Dare, Kehinde O. Ogunniran, Tolutope O. Siyanbola, Anuoluwa A. Akinsiku, Cyril O. Ehi-Eromosele, Christiana O. Ajanaku and Winifred U. Anake

Abstract— A versatile route to synthesize polymer based and polyol mediated silver nanoparticles with tunable morphological properties was evolved. Novel three dimensional (3D) quasi nanocubes, one dimensional (1D) nanorods and (2D) nanorods were produced by rapid solution phase transformation of silver sol with hot addition of absolute ethanol or toluene. The optical characterization showed existence of plasmon resonance band occurring in all cases. The electron micrographs revealed that the shape, size and size distribution of as prepared silver nanoparticles depended on the stabilizer or capping agent, mole ratio of metal ion sources, temperature and time of reaction.

Index Terms— silver nanoparticles, polyol, capping agent, surface plasmon resonance, stabilizer

1 INTRODUCTION

IN recent times, concerted effort has been made to synthesize diverse range of silver nanoparticles varying in size, geometry, and morphology because of their potential applications, particularly in electronics [1], electrochemical sensing [2], catalysis [3], and antimicrobial properties [4]. The size, geometry, dispersion and stability often determine the suitability of the nanoparticles for certain applications. Synthesis may involve physical means such as ultraviolet light, microwaves, photoreduction, or chemical reduction using hydrazine, ascorbic acid, sodium borohydride, glucose, and organic stabilizers.

The wet chemical processes generally involve the reduction of silver ions in water with an organic co-solvent or reducing agent such as dimethyl formamide (DMF) [5], [6] and methanol.. When a homogeneous dispersion is important, a suitable organic stabilizer, generally with strong electron-donating groups for metal surfaces, is often required. The literature describes the use of various polymeric forms of stabilizers, including linear, dendritic and comb-like polymers, because of their ability to interact with metal particles. And examples often include amphiphilic polymers with functional groups such as carboxylate [7], [8], imine, amide and poly(oxyethylene) [9]. These dispersants have been shown to be able to produce homogeneous aqueous dispersions of Ag NPs with particle sizes less than 20.0 nm [10].

Herein, we report synthesis of silver nanoparticles, reducing silver ions present in the aqueous and non-aqueous solutions of silver nitrate in different polymer and surfactant matrices.

- *Joseph A. Adekoya, Ph.D (Chemistry), Covenant University, Nigeria, PH-+2348056532188. E-mail: joseph.adekoya@covenantuniversity.edu.ng*
- *Enock O. Dare, Ph.D (Chemistry),Federal University of Agriculture, Abeokuta, Nigeria, E-mail: dare3160@hotmail.com*
- *Kehinde O. Ogunniran, Ph.D (Chemistry), Covenant University, Nigeria, E-mail: kehinde.ogunniran@covenantuniversity.edu.ng*
- *Tolutope O. Siyanbola, Ph.D (Chemistry), Covenant University, Nigeria, E-mail: tolu.siyanbola@covenantuniversity.edu.ng*
- *Anuoluwa A. Akinsiku, M.Sc (Chemistry), Covenant University, Nigeria, E-mail: anu.akinsiku@covenantuniversity.edu.ng*

2 MATERIALS

All inorganic salts, solvents and chemical reagents used were analar grade, and were purchased from Sigma-Aldrich Corporation, UK. They are as follow: silver nitrate, sodium borohydride, glycerol (GLY), ethylene glycol (EG), diethylene glycol (DEG), pentaerythritol (PET), trisodium citrate (SC), hexadecylamine (HDA), trioctylphosphine (TOP), poly(vinyl pyrrolidone) (PVP), toluene, methanol and ethanol.

2.1 Experimental

Monodispersed Ag nanoparticles were prepared according to Toshima *et al*. [11] as follows: 10 mL glycerol (99.5 % w/w) was measured into a round bottom flask containing a magnetic stirrer, 0.03-0.05 mmol PVP was added. Then the mixture was continuously stirred and gradually heated at the rate of 1.8^{0}C/min. to 160^{0}C. Afterward, 0.58-1.18 mmol $AgNO_3$ was added to the hot solution and the reaction was continued for 2 hours with continuous stirring. After the hot injection of silver nitrate, a yellow coloured silver sol was obtained as the temperature was maintained till the completion of reaction. The cooled yellow coloured Ag sol was copiously washed several times with methanol, and then centrifuged at 4400 rpm for 10-15 min. to remove excess unreacted polymer. The Ag sol was later redispersed in ethanol. The proposed scheme of reaction is given below. The above procedure was repeated at (i) 175^{0}C, 2 hours, (ii) using ethylene glycol at 175^{0}C, 2h and (iii) diethylene glycol at 190^{0}C, 2h. The difference in colour indicates the formation of different nanostructures of Ag nanoparticles.

Subsequently, 37.14 mmol pentaerythritol (PET) was added to 0.04-0.07 mmol PVP in 100 mL Milliken deionised H_2O according to the above procedure. The mixture was continuously stirred and dissolved, followed by gradual heating at the rate of 1.0^{0}C/min to 90^{0}C. Afterward, 1.17-1.38 mmol $AgNO_3$ was added to the solution, followed by hot injection of 10 mL, 5.39 mM $NaBH_4$. The reaction was continued for 2 hours with continuous stirring. The resulting cooled yellow coloured Ag sol was copiously washed with deionised H_2O and centrifuged at 4400 rpm for 10-15 min. to remove excess

unreacted polymer. The Ag sol was later redispersed in deionised H_2O. Again, the same procedure was repeated using 1.28 mmol, trisodium citrate (SC) as capping ligand to give SC capped Ag nanoparticles.

So also, 25.59 mmol HDA was slowly heated at the rate of 2.2^{0}C/min. to 200^{0}C with continuous stirring. Then 0.60 mmol $AgNO_3$ dispersed in 10 mL TOP was added, followed by hot injection of 5 mL glycerol to produce HDA capped Ag nanoparticles. This was washed with methanol several times, centrifuged and dispersed in toluene. The centrifuged sols obtained after decantation was redispersed in double distilled ethanol and cleaned in ultrasonic bath at 50^{0}C for 60 minutes before further characterization.

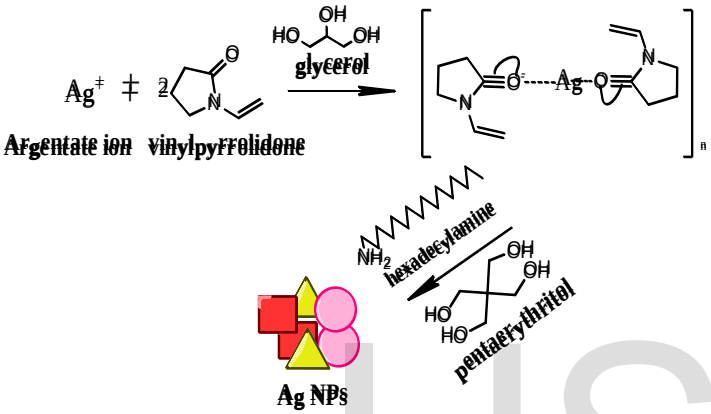

Scheme of Reaction for Ag Nanoparticle in PVP Stabilizing medium with glycerol, hexadecylamine and pentaerythritol as reductants

2.2 Characterization

The nanoclusters derived by thio stabilization were very found to be stable in both liquid and solid phases. The stability was checked by following the absorbance spectra over extended periods of several months. The use of sodium borohydride resulted in fast reduction of metal ions, but ethane-1, 2-diol, glycerol and diethylene glycol provided the solvent media and also offered relatively optimum reduction potential, while dodecanethiol was used as a stabilizer. The oxo groups present in the vinylpyrrolidone coordinate rather fairly strongly to the bimetallic nanoparticles [11], [12]. A wide variety of techniques such as UV-Visible spectroscopy, photoluminescence spectroscopy, TEM, XRD, and XPS were used for the characterization of as prepared Ru and Ag/Ru nanoparticles.

2.2.1 Optical Characterization

A Varian Cary 50 Conc UV-Visible spectrophotometer was used to carry out the optical measurements and the samples were placed in silica cuvettes (1 cm path length), using toluene as a reference solvent. A Perkin-Elmer LS 55 Luminescence spectrometer was used to measure the photoluminescence of the particles. The samples were placed in a quartz cuvette (1 cm path length).

2.2.2 Structural characterization

The crystalline phase was identified by X-ray diffraction (XRD), employing a scanning rate of 0.05^o min^{-1} in a 2θ range from 20 to 80^o, using a Bruker AXS D8 diffractometer equipped with nickel filtered Cu Kα radiation (λ = 1.5406 Å) at 40 kV, 40 mA and at room temperature. The morphology and particle sizes of the samples were characterized by a JEOL 1010 TEM with an accelerating voltage of 100kV, Megaview III camera, and Soft Imaging Systems iTEM software. The detail morphological and structural features were investigated using HRTEM images with a JEOL 2010 transmission electron microscope operated at an accelerating voltage of 200 kV.

3 RESULTS AND DISCUSSION

3.1 Optical Spectra of Ag Nanoparticles

The synthesis of monometallic Ag nanoparticles by chemical reduction in solution was carried out under different reaction conditions. The particles were characterised by active light absorption in the wavelength range of 400-440 nm indicating complete reduction of Ag(I) ion [13], which corresponded to Ag surface plasmon peak and confirmed the metallic nature of the nanoparticles [14]. The combined UV-Visible spectra of Ag sols for all these reaction conditions are shown in Figs. 1 and 2.

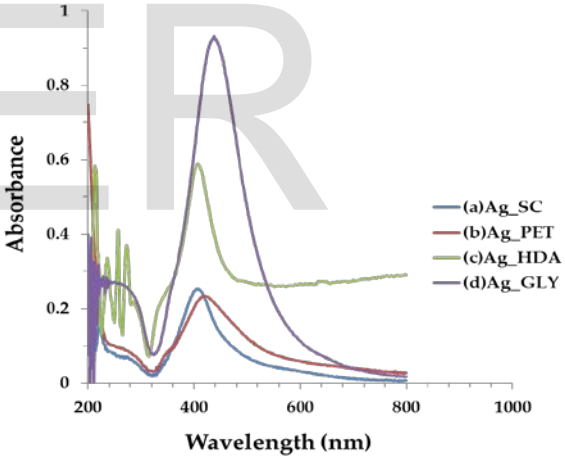

Fig. 1: UV-Vis Spectra of Ag sols stabilized with (a) PVP/SC at 90^{0}C, 2h (b) PVP/PET at 90^{0}C, 2h (c) HDA/GLY at 200^{0}C, 2h (d) PVP/GLY at 175^{0}C, 2h

In each of these reactions, polymer and surfactant stabilized Ag nanoparticles were prepared from various mole ratios of metal salt precursor to PVP/surfactant. At these combining ratios there were no precipitations, and a deep yellow sol was formed in all cases confirming the reduction of Ag^+ ion. However, SC surfactant stabilized Ag nanoparticles exhibited maximum absorbance at a relatively lower wavelength of 402 nm which in principle indicated the existence quantum size confinement.

The surface plasmon resonance band was a dominant feature of the synthesized Ag nanoparticles. Its position varied for each PVP/polyol or PVP/capping agent stabilized Ag nanoparticles. The PET and HDA stabilized Ag sols exhibited narrow peaks and were blue shifted to 420 and 402 nm respec-

IJSER

tively. As a result, both the shape and size of the silver particles experienced quantum confinement effect. Infact, monodispersed spherical shape has been reported for blue shifted wavelength near 400 nm [15], while rods were reported at higher wavelength above 420 nm [16] with a broad peak and lower extinction coefficient as seen in glycerol stabilized Ag nanoparticles, AgGLY at 160^{0}C, 2h.

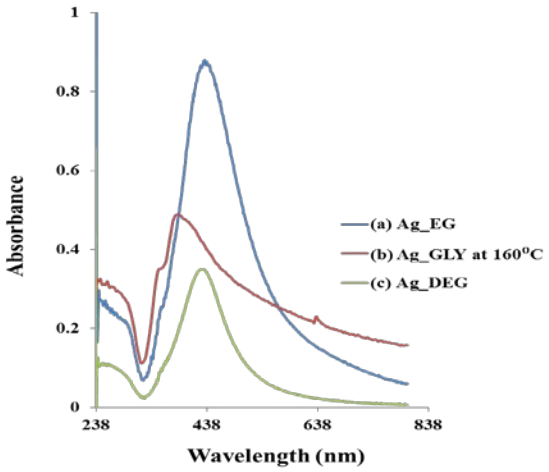

Fig. 2: UV-Vis Spectra of Ag sols stabilized with (a) PVP/EG at 175°C, 2h (b) PVP/GLY at 160°C, 2h (c) PVP/DEG at 190°C, 2h

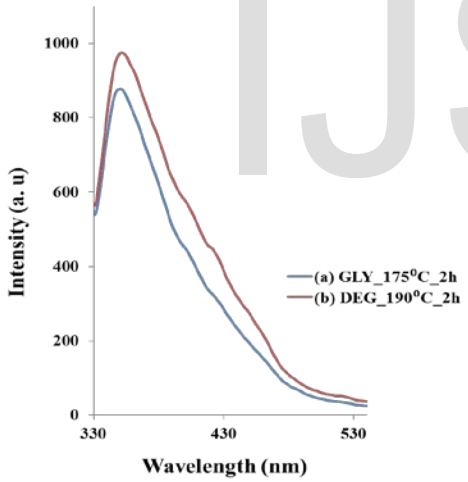

Fig. 3: PL emission spectra of (a) Ag GLY at 175^{0}C, 2h; (b) Ag DEG at 190^{0}C, 2h excited at 315 nm both exhibited emission at 347 and 700 nm double frequencies

Ag nanoparticles exhibit very unique and tunable optical properties on account of their surface plasmon resonance (SPR) influenced by shape, size and temperature of reaction. The refractive index of the solvent medium also has been shown to induce a shift of the surface plasmon band (SPB) as predicted by Mie theory [17]. The maximum wavelength for a given metal cluster depends on the refractive index of the medium and it shifts to higher wavelength as refractive index of the solvent increases [18], [19], [20]. The long tail absorption along with the 402 nm band indicates the anisotropic nature of Ag nanoparticles, while the long tail absorption is due to longitudinal SPR absorption [21].

The absorption band gaps of the Ag sols were also estimation by the direct band gap method [22] using the cut-off band edges (Figure 1), and were found to be 2.76 eV (448.90 nm, t = 2h), 2.87 eV (432 nm, t = 2h), 2.90 eV (427 nm, t = 3h), 2.89 eV (428.98 nm, t = 2h), 3.05 eV (406 nm, t = 2h) and 3.09 eV (402 nm, t = 4h) for PVP/GLY, PVP/DEG, PVP/EG, PVP/PET, PVP/SC and HDA/GLY functionalized Ag nanoparticles respectively. The absorption edges were red-shifted from that of Ag bulk crystals given as 3.99 eV [23], [24].

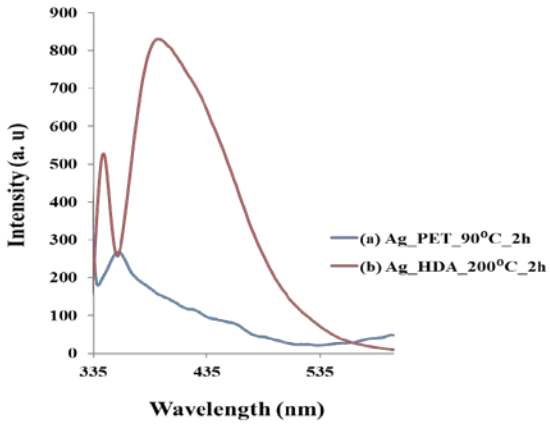

Fig. 4: PL emission spectra of (a) Ag PET at 90^{0}C, 2h; (b) Ag HDA/GLY at 200^{0}C, 2h excited at 330 and 340 nm respectively, both exhibited emission at 355 and 386 nm respectively

The photoluminescence spectra of Ag clusters in polyols and organic capping agents are presented in Figs. 3 and 4. There was a clear evidence of stoke's shift [25], that is, S_1-S_0 transition which accounted for the loss of energy between excitation and emission of fluorophores. In the case of Ag sols stabilized with DEG and GLY (Fig. 3) emission took place at 347 nm (3.57 eV) for excitations at 315 and 320 nm. This symmetry strongly suggested the occurrence of fluorescence and monodispersity of Ag clusters and clearly indicated the presence of very small Ag nanoparticles in the sols [26], [27]. The intense and narrow emission peaks as well as the quantum yield were characteristic of Ag nanoclusters, making it a potential material for sensor application. But it was also observed that S_1-S_0 emission took place at 394 nm for excitation at 340 nm in HDA/GLY stabilized Ag sol (Fig. 4), while PVP/PET stabilized Ag sol (Fig. 4) exhibited emission at 355 nm for a uniform excitation at 310 and 330 nm. The different emission wavelengths of Ag nanoparticles in different media could be due to solvent effect [28]. The emission which occurred at longer wavelength corresponded to lower energy.

A relationship was also established for the synthesis of silver nanoparticles, between the optimum mole ratio of metal precursor and stabilizer/surfactant medium needed to precipitate the Ag sols. For instance, it was found that the stoichiometry ratio of 47:1, 29:1:32, 19:1:531 and 1:43 for Ag/PVP$_{GLY}$, Ag/PVP/SC/$_{aq}$, Ag/PVP/PET/$_{aq}$ and Ag/HDA$_{GLY}$ mixtures respectively produced true dispersions in ethanol which gave the optical activity observed. In this order, HDA appeared to be the most effective because of the mole of Ag

IJSER

precursor required to form the sol.

3.2 Morphology of Ag nanoparticles

The transmission electron micrographs of Ag clusters in different stabilizing media are presented in Figs. 5 -.8 confirming the polydispersed nature of Ag nanoparticles which were formed, thus, establishing the anisotropy of nanoparticles formation. The images also revealed that different shapes and dimensions of silver nanostructures were formed. The temperature of reaction noticeably played a key role in the size and growth pattern of Ag nanoparticles in different media. It was particularly observed that the polycrystallinity of PVP/EG stabilized Ag nanoparticles (Fig. 5a, b, 6a, b) increased with temperature and reaction time.

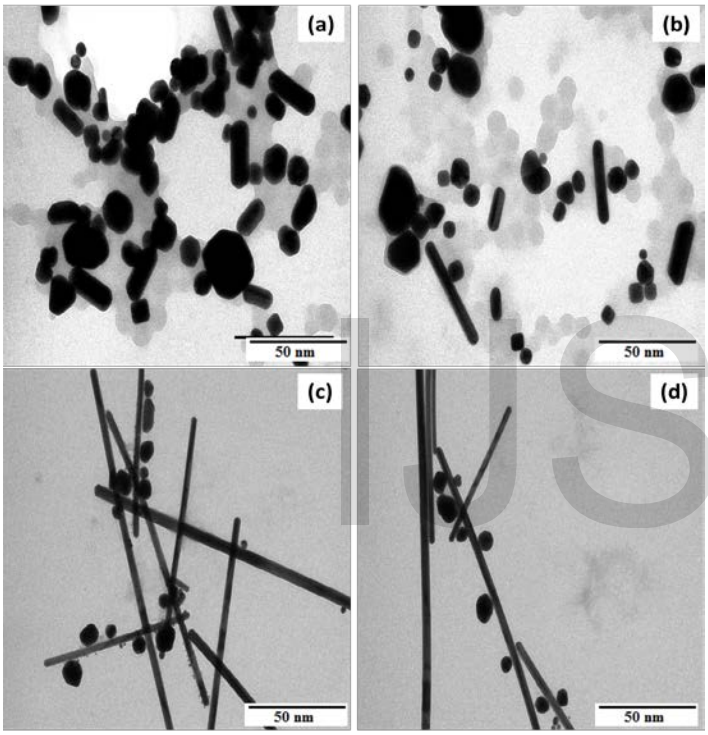

Fig. 5: TEM micrographs of Ag nanoparticles stabilized with (a, b) PVP/EG at 175^{0}C, 2h; (c, d) PVP/GLY at 160^{0}C, 2h showing tunable 2D and 3D quantized morphology

The different shapes observed are rod, cube and truncated edge cube. In PVP/EG stabilized Ag nanocluster prepared at 175^{0}C, 2h (Figure 5a, b) the mean length of nanorods and 3D quantized nanocubes is 22.9±1.2 nm, the mean diameter of the rods is 17.5±1.5 nm. Whereas the size and shape of silver nanoparticles obtained in the same stabilizer at 160^{0}C, 2h (Figure 6a, b) showed no significant difference. As for PVP/GLY stabilized Ag nanoclusters, prepared at 160^{0}C, 2h (Figure 5c, d) the mean size of 3D quantized cubes is 18.8±2.4 nm, while the short rods have a mean length of 42.6±13.75 nm and the long ones have an average of 150±64.5 nm. The growth pattern of the rod is suggested to be by longitudinal attachment via the initial nuclei formed at the beginning of nucleation [29]. The HDA/GLY capped Ag nanocluster formed at 200^{0}C, 2h (Figure 7a) resulted in monodispersed nanocubes showing a periodic array (Figure 7b) with a mean size of 17.5±3.3 nm. The effect of quantum size confinement and the monodisperse nature of the nanoparticles formed can be said to be as a result of the aliphatic multiple N-bearing ligand [30] which controlled the nucleation and growth of nanocubes. In addition, etching due to the presence of oxygen and other electronegative species in the reaction mixture contributed significantly to the controlled reduction of Ag^+ to Ag^0 [31].

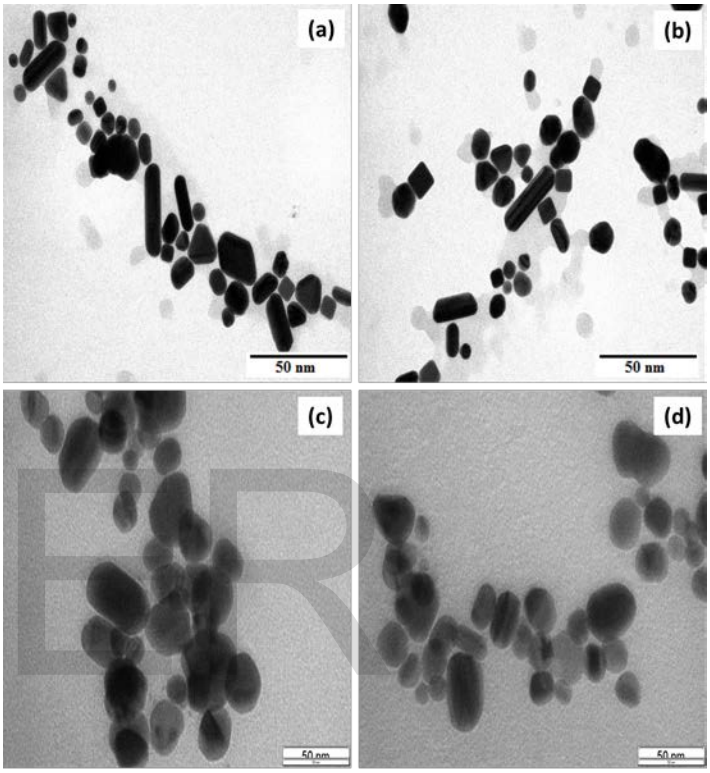

Fig. 6: TEM micrographs of Ag nanoparticles stabilized with (a, b) PVP/EG at 160^{0}C, 2h; (c, d) PVP/PET at 90^{0}C, 2h showing tunable morphology and monodispersity

In the aqueous phase, PVP/SC stabilizer produced quassi cube shaped monodispersed Ag nanoparticles at 90^{0}C, 2h (Figure 7c, d), with a mean diameter of 19.71±1.6 nm. While the aqueous phase PVP/PET functionalized Ag nanocluster formed at 90^{0}C, 2h (Figure 6c, d) gave mean sizes of cube and rod equivalent to 20.2±4.3 and 27.9±4.5 nm respectively. It was observed that the morphology of Ag nanoparticles was different in aqueous and organic phases. The ripening process was largely surfactant or stabilizer dependent. The HRTEM micrographs of Ag nanocluster stabilized with PVP/SC (Figure 8a) showed its crystallinity by several overlapping lattice fringes of approximately 2.33 Å in the micrograph. All these confirm that the morphology of Ag nanoclusters can be tunable using different surfactant or stabilizers, and that the growth of Ag nanoclusters is also temperature dependent.

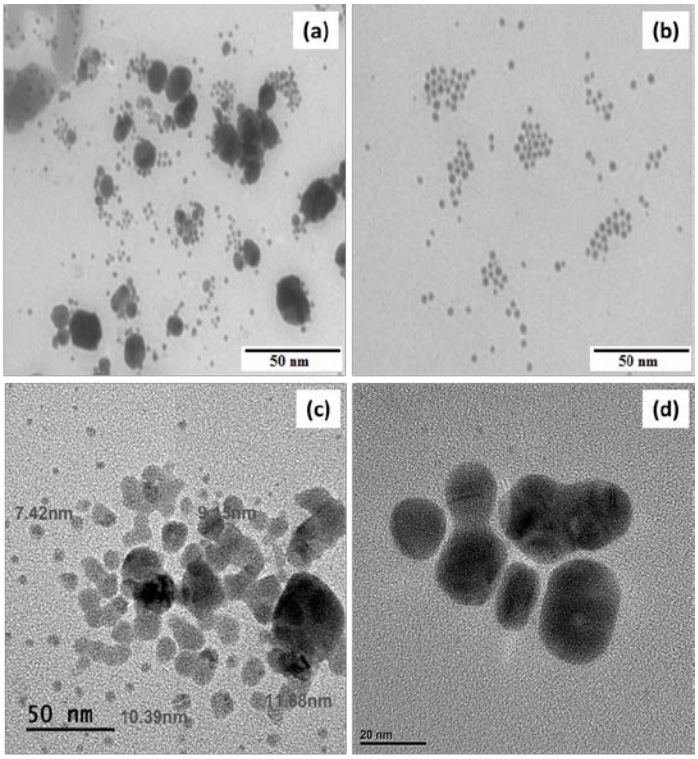

Fig. 7: (a, b) TEM Images of Ag NPs stabilized with HDA/GLY at 200^{0}C, 2h showing its monodispersity; (c, d) HRTEM Micrographs of Ag NPs stabilized with PVP/SC at 90^{0}C, 2h showing formation of nanocubes

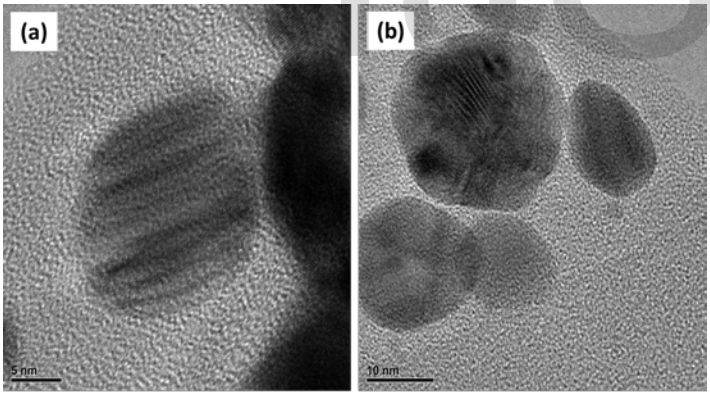

Fig. 8: (a, b) HRTEM Micrographs of Ag NPs stabilized with PVP/SC at 90^{0}C, 2h showing clear lattice fringes and truncated edge nanocubes

The p-XRD patterns of a typical silver nanoparticle synthesized in this study are almost identical irrespective of the experimental conditions (Figure 9), which is an indication of high degree of crystallinity. For instance, HDA/GLY capped Ag nanoparticles (Figure 9b) gave well refined reflections at 2θ: 38.19^0, 44.28^0, 64.51^0 and 77.50^0 corresponding to {111}, {200}, {220} and {311} crystallographic planes which can be readily indexed to face-centered cubic (fcc) silver with a calculated lattice constant of 2.3 Å [32]. Their sizes were calculated at (100) diffraction plane using the Scherrer equation and were found to be: Ag PVP/DEG, 14.68 nm; Ag PVP/GLY, 21.07 nm; Ag PVP/EG, 25.56 nm; Ag HDA/GLY, 21.33 nm; Ag PVP/SC, 20.66 nm; and Ag PVP/PET, 16.64 nm. These values to a large extent agree with TEM measurements.

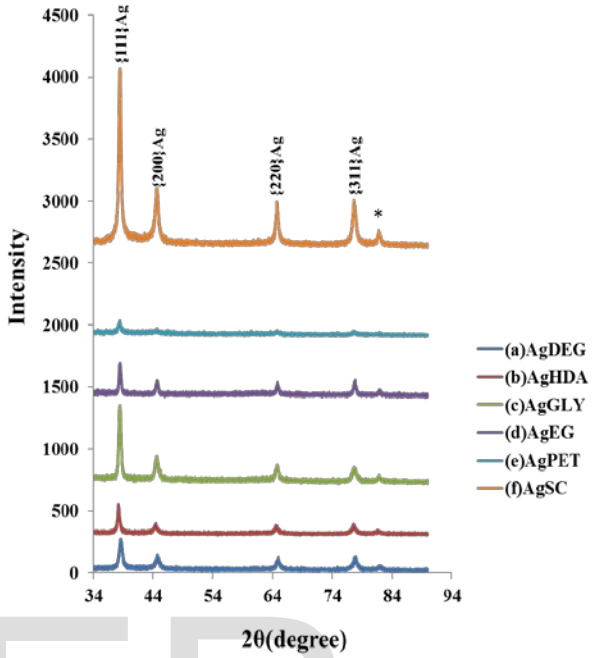

Fig. 9: XRD Patterns of Ag nanoparticles stabilized with (a) PVP/DEG; (b) HDA/GLY; (c) PVP/GLY; (d) PVP/EG; (e) PVP/PET and (f) PVP/SC

4.0 CONCLUSION

The synthesis of silver nanoparticles by wet chemical reduction and precipitation from non-aqueous and aqueous solutions using molecular source precursors and encapsulation matrices has been accomplished. Subsequently, characterization of the prepared nanoparticles was done using optical spectrometry, electron microscope and x-ray diffractometer (XRD). The functionalized Ag particles obtained showed evidence of being nanostructured based on size, shape, distribution and morphology. Their optical characterization portends electronic and morphological properties that can be exploited for fibre optic and sensing applications.

5.0 ACKNOWLEDGEMENTS

The authors are grateful to the National Research Foundation (NRF) and the Department of Science and Technology (DST) South Africa. The authors also thank Dr. James Wesley-Smith of the Electron Microscopy Unit, University of Kwa-Zulu Natal for electron microscopy (TEM) measurements and CSIR, Pretoria for HRTEM facility.

6.0 REFERENCES

[1] P. V. Kamat, Photophysical, photochemical and photo catalytic aspects of metal nanoparticles. *J Phys Chem B*, 2002; 106: 7729–44.

[2] L. M. Liz-Marzán, Tailoring surface plasmons through the morphology and assembly of metal nanoparticles. Langmuir 2006; 22: 32–41.

[3] F. Zhang, Y. Pi, J. Cui, X. Zhang, N. Guan. Unexpected selective photocatalytic reduction of Nitrite to nitrogen on silver-doped titanium dioxide. *J. Phys. Chem. C* 2007; 111: 3756–61.

[4] T. Sakai and P. Alexandridis (2006). Ag and Au monometallic and bimetallic colloids: morphogenesis in amphiphilic block copolymer solutions. *Chemical Materials* 2006; 18, 2577–2583.

[5] I. Sondi, D. V. Goia, E. Matijevic. Preparation of highly concentrated stable dispersions of uniform silver nanoparticles. *J Colloid Interface Sci*., 2003; 260:75–81.

[6] A. Panácek, L. Kvítek, R. Prucek, M. Kolár, R. Vecerová, N. Pizúrová, et al. Silver colloid nanoparticles: synthesis, characterization, and their antibacterial activity. *J Phys Chem B*, 2006; 110: 16248–53.

[7] I. Pastoriza-Santos and L. M. Liz-Marzán. Synthesis of silver nanoprisms in DMF.Nano Lett 2002; 2:903–5.

[8] G. Nesher, G. Marom and D. Avnir. Metal–polymer composites: synthesis and characterization of polyaniline and other polymer at silver compositions. *Chem Mater.,* 2008; 20: 4425–32.

[9] C. E. Hoppe, M. Lazzari, I. Pardiñas-Blanco and M. A. López-Quintela, One Step Synthesis of Gold and Silver Hydrosols Using Poly (N-vinyl-2pyrrolidone) as a reducing agent. *Langmuir,* 2006; 22, 7027–7034.

[10] Y. Zhang, H. Peng, W. Huang, Y. Zhou, X. Zhang and D. Yan, Hyper-branched Poly(amidoamine) as the stabilizer and reductant to prepare colloid silver nanoparticles in situ and their antibacterial activity. *Journal of Physical Chemistry C* 2008; 112, 2330-2336.

[11] N. Toshima, M. Kanemaru, Y. Shiraishi and Y. Koga, Spontaneous Formation of Core/Shell Bimetallic Nanoparticles: A Calorimetric Study. *The Journal of Physical Chemistry B* 2005; 109 (24), 16326-16331.

[12] N. Toshima, K. Kushihashi, T. Yonezawa and H. Hirai, Colloidal dispersion of palladium-platinum bimetallic clusters protected by polymers, preparation and application to catalysis. *Chem. Lett.* 1989; 18 (10), 1769-1772.

[13] P. Raveendran, J. Fu and S. L. Wallen, A simple and green method for the synthesis of Au, Ag, and Au–Ag alloy nanoparticles. *Journal of Green Chemistry* 2006; 8, 34–38.

[14] G. B. Sergeev, Nanochemistry of Metals. *Russian Chemical Review*, 70 (10) 2001; 809-825.

[15] S. Link, Z. L. Wang, and M. A. El-Sayed, Alloy formation of Gold-Silver nanoparticles and the dependence of the Plasmon Absorption on their Composition. *Journal of Physical Chemistry B* 1999; 103, 3529-3533.

[16] D. Rui-Xuan, T. Wei-Cheng and L. Jiang-Jen, Tandem synthesis of silver nanoparticles and nanorods in the presence of poly(oxyethylene)-amidoacid template. *European Polymer Journal* 2011; 47, 1383–1389.

[17] R. Wargnier, A. V. Baranov, V. G. Maslov, V. Stsiapura, M Artemyev, M. Pluot, A. Sukhanova, and I. Nabiev, Energy transfer in aqueous solutions of oppositely charged CdSe/ZnS core-shell quantum dots and in quantum dot-nanogold assemblies. *Nanotechnology Letter,* 2004; 4(3), 451–457.

[18] A. Ingle, A. Gade, S. Pierrat, C. Sonnichsen and Rai, M. Mycosynthesis of silver nanoparticles using the fungus Fusarium acuminatum and its activity against some human pathogenic bacteria. *Current Nanoscience*, 2008; 4, 141–144.

[19] A. C. Templetou, J. J. Pletron, R. W. Murray and P. Mulvaney, Solvent refractive Index and Core Charge Influences on the surface Plasmon Absorbance of Alkanethiolate monolayer Protected Gold clusters. *Journal of Physical Chemistry B*, 2000; 101, 564-570.

[20] S. Underwood and P. Mulvaney, Effect of the solution refractive index on the colour of gold colloids. *Langmuir,* 1994; 10, 3427–3430.

[21] L. Gou, M. Chipara, and J. M. Zaleski, Convenient, rapid synthesis of Ag nano-wires. *Chemistry of Materials* 2007; 19, 1755–1760.

[22] M. Hoffman, S. Martin, W. Choi, and D. Bahnemann, "Environmental applications of semiconductor photo catalysis," *Chemical Review,* 1995; **95**, 69-96.

[23] K. Seok-Soon, N. Seok-In, J. Jang, K. Dong-Yu and N. Yoon-Chae, Plasmon enhanced performance of organic solar cells using electrodeposited Ag nanoparticles. *Applied Physics Letters*, 2008; **93**, 073307-1-3.

[24] *A. Koichi, F. Makoto, R. Carsten, T. Junji, M. Hirotaka, O. Yoshimichi, Y. Naoya and W. Toshiya, A Plasmonic Photocatalyst Consisting of Silver Nanoparticles Embedded in Titanium Dioxide.* Am. Chem. Soc., *2008; 130 (5), 1676–1680.*

[25] R. F. Wang, H. Wang, B. X. Wei, W. Wang, and Z. Q. Lei, Carbon supported Pt shell modified PdCo core with electrocatalysts for methanol oxidation. *International Journal of Hydrogen Energy*, 2010; **35,** 10081-10086.

[26] L. Chunhua, Y. Xiupei, Y. Hongyan, Z. Zaide and X. Dan, Preparation of Silver Nanoparticle and Its Application to the Determination of ct-DNA. *Sensors,* 2007; 7, 708 -718.

[27] A. Ledo-Suárez, J. Rivas, C. F. Rodríguez-Abreu, M. J. Rodríguez, E. Pastor, C. A. Hernández, S. B. Oseroff and M. A. López-Quintela, Facile Synthesis of Stable, Sub-Nanosized Silver Atomic Clusters in Microemulsions. *Catch Phrase,* 2008; DOI: 10.1002/anie.200.

[28] J. H. Liu, A. Q. Wang, Y. S. Chi, H. P. Lin and C. Y. Mou, Synergistic effect in an Au–Ag alloy nanocatalyst: CO oxidation, *Journal of Physical Chemistry B,* 2005; 109, 40-43.

[29] R. P. Andres, R. S. Averback, W. L. Brown, L. E. Brus, W. A. Goddard, A. Kaldor, S. G. Louie, M. Moscovits, P. S. Peercy, S. J. Riley, R. W. Siegel, F. Spaepen and Y. Wang, Research opportunities on clusters and cluster-assembled materials A Department of Energy,

Council on Materials Science Panel Report. *Journal of Material Resources* 1989; 4, 704–736.

[30] D. Bartczak, and A. G. Kanaras, Diacetylene-Containing ligand as a new capping agent for the preparation of water-soluble colloidal nanoparticles of remarkable stability. *Langmuir*, 2010; 26, 7072-7077.

[31] S. S. Datta, Wetting and energetics in nanoparticle etching of grapheme. *J. Appl. Phys*., 2010; 108, 024307

[32] E. O. Dare, O. W. Makinde, K. T. Ogundele, G. A. Osinkolu, Y. A. Fasasi, I. Sonde, J. T. Bamgbose, M. Maaza, J. Sithole, F. Ezema, and O.O. Adewoye, Zinc Salt-Mediated Synthesis, Growth Kinetic and Shaped Evolution of Silver Nanoparticles. *International Scholarly Research Network ISRN Nanomaterials* 2012;doi:10.5402/2012/376940.

- *Cyril O. Ehi-Eromosele, M.Sc (Chemistry), Covenant University, Nigeria, E-mail: cyril.ehi-eromosele@covenantuniversity.edu.ng*
- *Christiana O. Ajanaku, M.Sc (Chemistry), Covenant University, Nigeria, E-mail:oluwatoyin.ajanaku@covenantuniversity.edu.ng;*
- *Winifred U. Anake, M.Sc (Chemistry), Covenant University, Ni-geria, E-mail:Winifred.anake@covenantuniversity.edu.ng*

*Corresponding author

IJSER